JTTEE5 18:678–685
DOI: 10.1007/s11666-009-9394-2
1059-9630/$19.00 © ASM International

Preparation and Characterization of $CaO-ZrO_2-SiO_2$ Coating for Potential Application in Biomedicine

Youtao Xie, Xuebin Zheng, Chuanxian Ding, Wanyin Zhai, Jiang Chang, and Heng Ji

(Submitted April 15, 2009; in revised form July 20, 2009)

In this paper, chemically synthesized $CaO-ZrO_2-SiO_2$ (CZS) powder was plasma sprayed onto a Ti-6Al-4V alloy substrate for its potential applications in biomedicine. Surface morphology and phase composition were analyzed by scanning electron microscopy (SEM) and x-ray diffraction (XRD). The degradation behavior of the coating in biological environment was in vitro appraised in Tris-HCl buffer. The mass loss was much lower than that of the wollastonite coating (WC) and close to that of the hydroxylapatite coating (HC). The bond strength with titanium alloy substrate was 31.8 ± 4.7 MPa. In vitro bioactivity appraisement results showed that apatite could be formed on the surfaces after soaking in simulated body fluid (SBF) for 14 days. Canine marrow stem cells (MSCs) also showed well adhesion and proliferation on the coating surfaces. In summary, results suggest that the coating possesses well cytocompatibility and may be an appropriate candidate for application in biomedicine.

Keywords $CaO-ZrO_2-SiO_2$, coating, marrow stem cells, plasma spraying

1. Introduction

Plasma-sprayed hydroxylapatite coating (HC) on a Ti-6Al-4V substrate has been widely used in orthopedics and dentistry to achieve chemical bonding of the implant to bone tissue (Ref 1). However, the low crystallinity and poor bonding strength result in degradation, peeling, and fatigue-induced failure under tensile loading (Ref 2, 3). Plasma sprayed $CaO-SiO_2$ based ceramic coatings have been widely studied recently for their high bonding strength with titanium substrate, good bioactivity and biocompatibility, but the degradation of the coatings in biological environment affects the long-term performance (Ref 4-6).

Good chemical and dimensional stabilities, mechanical strength and toughness, coupled with a Young's modulus in the same order of magnitude with stainless steel, were the origin of the interests in using zirconia as a ceramic biomaterial. Zirconia was also used as reinforcement in many types of ceramic because of its high strength and toughening characteristics during crack-particles interactions (Ref 7-10). Sintered composite of hydroxylapatite and zirconia was reported to have much higher mechanical properties than pure hydroxylapatite (Ref 11, 12). The strength and fracture toughness of bulk bioglasses containing zirconia were obviously enhanced (Ref 13) and degradation in vivo was mitigated (Ref 14). The good biocompatibility of zirconia ceramic was also been extensively proved (Ref 15). Human osteoblasts were found to spread, adhere to the material surface closely, and no any cytotoxicity was found (Ref 16, 17). However, as a bioinert material, most of the zirconia implant was generally encapsulated by fibrous tissue that isolated them from surrounding bone tissue (Ref 18).

Colin et al. (Ref 19) found that calcium oxide in calcia partially stabilized zirconia (Ca-PSZ) could react with acid oxides, such as silicon oxide, titania, and extracted from the zirconia matrix at high temperature. For example, the calcia can react with silicon or silicon oxide to form $CaSiO_3$ or Ca_2SiO_4 phase in the near zirconia zone. In this paper, a decalcification reaction of Ca-PSZ with silica was used to prepare the $CaO-ZrO_2-SiO_2$ (CZS) powder, which was plasma sprayed onto a titanium alloy substrate for potential application in biomedicine. The powder and coating surface morphologies and phase composition were evaluated by scanning electron microscopy (SEM) and x-ray diffraction (XRD). The bonding strength of the coating with titanium alloy substrate was measured. The degradation behavior in biological environment was in vitro appraised by monitoring the mass losses in Tris-HCl buffer. Cytocompatibility was evaluated by observing the attachment, proliferation behavior of canine marrow stem cells (MSCs) on the coating surface.

Youtao Xie, Xuebin Zheng, Chuanxian Ding, and **Heng Ji**, Key Laboratory of Inorganic Coating Materials, Chinese Academy of Science, Shanghai, China and Shanghai Institute of Ceramics, Chinese Academy of Science, 1295 Dingxi Road, Shanghai 200050, China; and **Wanyin Zhai** and **Jiang Chang**, Shanghai Institute of Ceramics, Chinese Academy of Science, 1295 Dingxi Road, Shanghai 200050, China. Contact e-mails: xieyoutao@mail.sic.ac.cn and xbzheng@mail.sic.ac.cn

2. Experimental

2.1 Feedstock and Coating Preparation

Commercially available pure ZrO_2 and $CaCO_3$ powder were mechanical mixed for 6-8 h in a polyethylene bottle with ethanol as media. The mixed powder were sintered in air at 1400 °C for 8-10 h in a muffle furnace with the heating rate at 5 °C min^{-1}. Then, silica powder was mechanically mixed into and the mixture was sintered in air at 1400 °C for another 10-14 h to obtain the CaO-ZrO_2-SiO_2 (CZS) ceramic. All of the original powders were analytical-reagent grade and obtained from Shanghai AiBi Chemistry Preparation Co, China. Combining the CaO-ZrO_2-SiO_2 phase diagram and the previous results (Ref 5), which reported that the dicalcium silicate/zirconia composite coatings with no more than 70 wt.% zirconia content exhibited good bioactivity and mechanical properties, the CaO-ZrO_2-SiO_2 ceramic in this study was prepared with the mole ratio of the $CaCO_3$:ZrO_2:SiO_2 at 1:1:0.4.

The obtained CZS ceramic was abrasive to less than 60 μm size as plasma spraying feedstock. Air plasma spraying (APS) system (Sulzer Metco, Switzerland) was employed to prepare the coating with Ti-6Al-4V plates (10 × 10 × 2 mm) as substrates. The detailed plasma spraying parameters are shown in Table 1.

2.2 Coating Characterization

The phases of the feedstock and coating were determined by x-ray diffraction (D/max 2550 v, Japan). The surface morphology and cross-sectional microstructure of the coating were evaluated by SEM coupled with an energy-dispersive spectrometer (EDS, INCA Energy, Oxford Instruments, UK). The porosity of the coating was estimated by image analysis techniques. Porosity level was determined by capturing an image of the coating cross-section and differentiating between porosity and bulk coating by grey levels. Surface roughness (Ra) of the coating was measured by a profilometer (Hommelwerke T8000-C, Germany). Bioactivity evaluation was performed by immersing the samples in simulated body fluid (SBF) with the ion concentrations similar to those in human blood plasma (Ref 20). The detailed composition of the SBF is shown in Table 2. After 14 days immersion, the samples were analyzed by SEM and EDS.

The degradation of the CZS coating in biological environment was in vitro evaluated by monitoring the mass losses of the coating after immersion in Tris-HCl buffer. Each piece of sample was immersed in 10 mL Tris-HCl buffer. After soaking for different periods, samples were washed by distilled water and alcohol and then dried at 105 °C for 24 h. The mass changes before and after soaking were measured. Mathematic average of the mass losses of five measurements was reported.

Table 1 Plasma spraying parameters

Argon plasma gas flow rate, slpm	40
Hydrogen plasma gas flow rate, slpm	10
Spray distance, mm	100
Argon powder carrier gas, slpm	3.5
Current, A	600
Voltage, V	68
Powder feed rate, g/min	21

Table 2 Ionic concentration of human blood plasma and SBF solution (obtained from calculation, unit: mM)

	Na^+	K^+	Ca^{2+}	Mg^{2+}	Cl^-	HCO_3^{2-}	HPO_4^{2-}	SO_4^{2-}
Human blood plasma	142	5.0	2.5	1.5	103.0	27	1	0.5
SBF solution	142	5.0	2.5	1.5	148.8	4.2	1	0.5

2.3 Bonding Strength Measurement

Two identical cylindrical Ti-6Al-4V rods (∅ 25.4 × 25.4 mm), one with coating (about 400 μm) and another was gritblast-roughened to enhance resin adherence were used according to designation of ASTM C633 (Ref 21). A thin layer of E-7 adhesive glue (Shanghai, China), whose tensile fracture strength is over 70 MPa, was used to bond the two cylinders together. In order to assure the intimate contact between the resin and the two surfaces, a compressive stress was applied to both rods for about 1-2 h before 4 h of curing at 100 °C in an oven. The tensile bonding strength was measured using a materials tester (Instron-5592, SATEC, USA) at a crosshead speed of 1 mm min^{-1}. The average of five test data was given to represent the bonding strength.

2.4 In Vitro Cytocompatibility

2.4.1 Cell Morphological Observation. Cells suspended in 200 μL Dulbecco's modified Eagle's medium (supplemented with 10% fetal bovine serum, 100 U mL^{-1} penicillin and 100 mg mL^{-1} streptomycin) at a density of 5×10^4 cells mL^{-1} (passage 5-7) were seeded on 1 cm^2 sample sterilized by autoclaving at 120 °C for 30 min. The culture was kept at 37 °C in an atmosphere of 5% CO_2 and 95% relative humidity. The culture medium was changed every other day. After cultivation for 2, 4, and 6 days, the samples were taken out from the culture plates and fixed with 2.5% glutaraldehyde in 0.1 M sodium cacodylate buffer (pH = 7.4) for 1 h. After rinsing with phosphate-buffered saline for three times, 10 min for each time, and dehydrating sequentially in a series of ethanol (50, 70, 95, and 100%), each concentration twice and 10 min for each time, the adhesion and spreading of the cells on the MS coating were observed by SEM.

2.4.2 MTT Assay. MTT assay was applied to determine the viability and proliferation of the MSCs. On complete removing of the original culture medium, 720 μL fresh culture media and 80 μL of MTT solution (5 mg mL^{-1}) were added to each well. The plate was incubated at the same cultivation condition for another 4 h. Then, an equal volume of the supernatant was removed carefully and the intracellular formazan was

solubilized by 800 μL of dimethyl sulfoxide for each well. The absorbance of the resulting solution was measured using spectrophotometry at a wavelength of 570 nm. The results were reported as absorbance which is proportional to the quantity of the living cells on the coating surface.

3. Results

3.1 Characteristics of the Coating

The phase composition of the sintered powder and as-sprayed coating is illustrated in Fig. 1. The feedstock was mainly composed of ZrO_2, Ca_2SiO_4 and $CaZrO_3$, while in the as-sprayed coating, the Ca_2SiO_4 phase peaks became weak since the decreased crystallinity of the coating in the rapid heating and cooling process of plasma spraying.

The surface morphologies of the as-sintered CZS powder and prepared coating are shown in Fig. 2(A)-(D). The coating showed typical characteristics of plasma spraying with rough surface. Higher magnification of the SEM micrographs showed that large amount of cuboid particles conglutinated together. EDS results demonstrated that the cuboid particles were ZrO_2.

The cross-sectional microstructure of the coating is shown in Fig. 3. Typical lamellar structure with a few pores can be seen from the images. Measured from the cross-sectional images, the thickness of the coating was about 80-100 μm and the porosity was approximately 9.8%. The measured bonding strength of the CZS coating with Ti-6Al-4V substrate is 31.8 ± 4.7 MPa, which is much higher than that of the plasma sprayed HC reported in some other studies (Ref 22, 23). Roughness (Ra) of the CZS coating is 6.92 ± 0.54 μm.

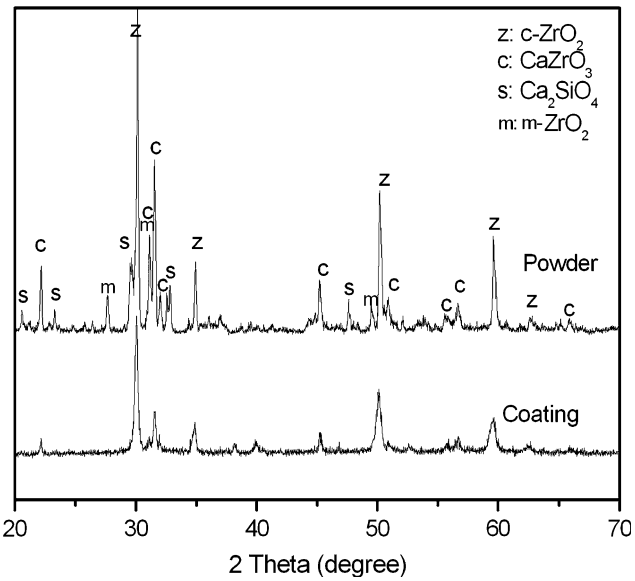

Fig. 1 XRD patterns of the as-sintered CZS powder and prepared coating

3.2 Dissolution Behavior in Tris-HCl Buffer

The degradation in biological environment was evaluated by monitoring the mass changes of the samples after immersion in Tris-HCl buffer. The surface morphology of the sample after immersion in buffer solution for 30 days is illustrated in Fig. 4. Results show that the cuboid zirconia particles remained after immersion in the buffer, and connected together to form a network. The further dissolution of the coating was therefore reduced. The dissolution percent of the coatings in the Tris-HCl buffer are shown in Fig. 5. It was 0.051 ± 0.021% for CZS after 5 days immersion, while that of the HC was 0.385 ± 0.041% and 2.88 ± 0.18% for WC.

3.3 In Vitro Bioactivity and Cytocompatibility Evaluation

To forecast the bone-bonding ability of the CZS coating, samples were immersed in SBF to test the bone-like apatite formation capability. After 14 days immersion in SBF, many island particles were formed on the sample surfaces as shown in Fig. 6. EDS measurements verified that these particles were mainly composed of Ca, P, O and a little of Na, Mg elements.

In vitro cytocompatibility was evaluated by canine MSCs culture system. HC and WC samples were fabricated for comparison. In order to exclude the influence of surface texture on the cells adhesion and proliferation, HC and WC samples were prepared with the roughness close to the CZS coating.

Figure 7 shows the cell morphologies after 2, 4, and 6 days culture on the CZS coating surface. Under SEM, large number of cells was observed to adhere to the material. These cells possessed a polygonal shape with many extending cytoplasmic processes adhering to the sample, spread and reached larger sizes with compact bodies and short cellular extensions. After 4 days of culture, the cells reached confluence on the coating surfaces.

The MTT results shown in Fig. 8 further demonstrated the well proliferation of the MSCs on CZS. The number of living cells increased with extending of culture time. During the 6 days culture, cells exhibited similar proliferation rate on both of CZS and HC.

4. Discussion

In this paper, a decalcification reaction between Ca-PSZ and silica at high temperature was employed for synthesis of CZS powder. The obtained powder showed a special microstructure: large amount of cuboid ZrO_2 particles conglutinated together with the interspace filled by silicate salts. Similar microstructure was also reported by Yeo et al. (Ref 24). This kind of structure is very beneficial for its potential application in biomedicine. The ZrO_2 particles are biocompatible and chemically stable in

biological environment, while the silicate salts, the bioactive dicalcium silicate, can induce the formation of apatite in SBF or biological environment. It indicates that the material can chemically bond to the host bone tissue and is of advantages to the early fixation of the implants (Ref 4, 5, 13, 17).

The degradation results evaluated in Tris-HCl buffer primary demonstrated the good stability of the coating. As shown in Fig. 4, after 30 days immersion in the buffer, the ZrO_2 particles remained in the coating and connected to form a network. The further reaction of water molecules with the silicate salts was reduced and thus the dissolution rate of the coating decreased. Therefore, the CZS coating showed a much lower dissolution rate as compared with WC.

The coating/substrate adhesion strength is one of the important factors in determining the performance and reliability of any coated devices in dental or orthopedic applications. Hydroxylapatite is the widely used material in biomedicine for its good bioactivity and biocompatibility. Unfortunately, the bonding strength with metal substrates is low because of the large difference in thermal expansion coefficients between the hydroxylapatite and substrate. In addition, as mentioned earlier (Ref 2, 3), the hydroxylapatite is degradable in the biological environment and the bonding strength between the coating and substrate largely declines with the extending of the implanting duration. For an ideal coating material in dental or orthopedic applications, not only good biocompatibility but also high bonding strength with substrate and low degradation rate in biological environment are needed. According to the dissolution results appraised in Tris-HCl buffer, smallest dissolution percent was found for CZS coating in the three kinds of material and a long life span could be expected after implanted.

The bonding strength of the CZS coating with Ti-6Al-4V substrate is 31.8 ± 4.7 MPa, which is much higher than that of the HC (Ref 22, 23). The high bonding strength of

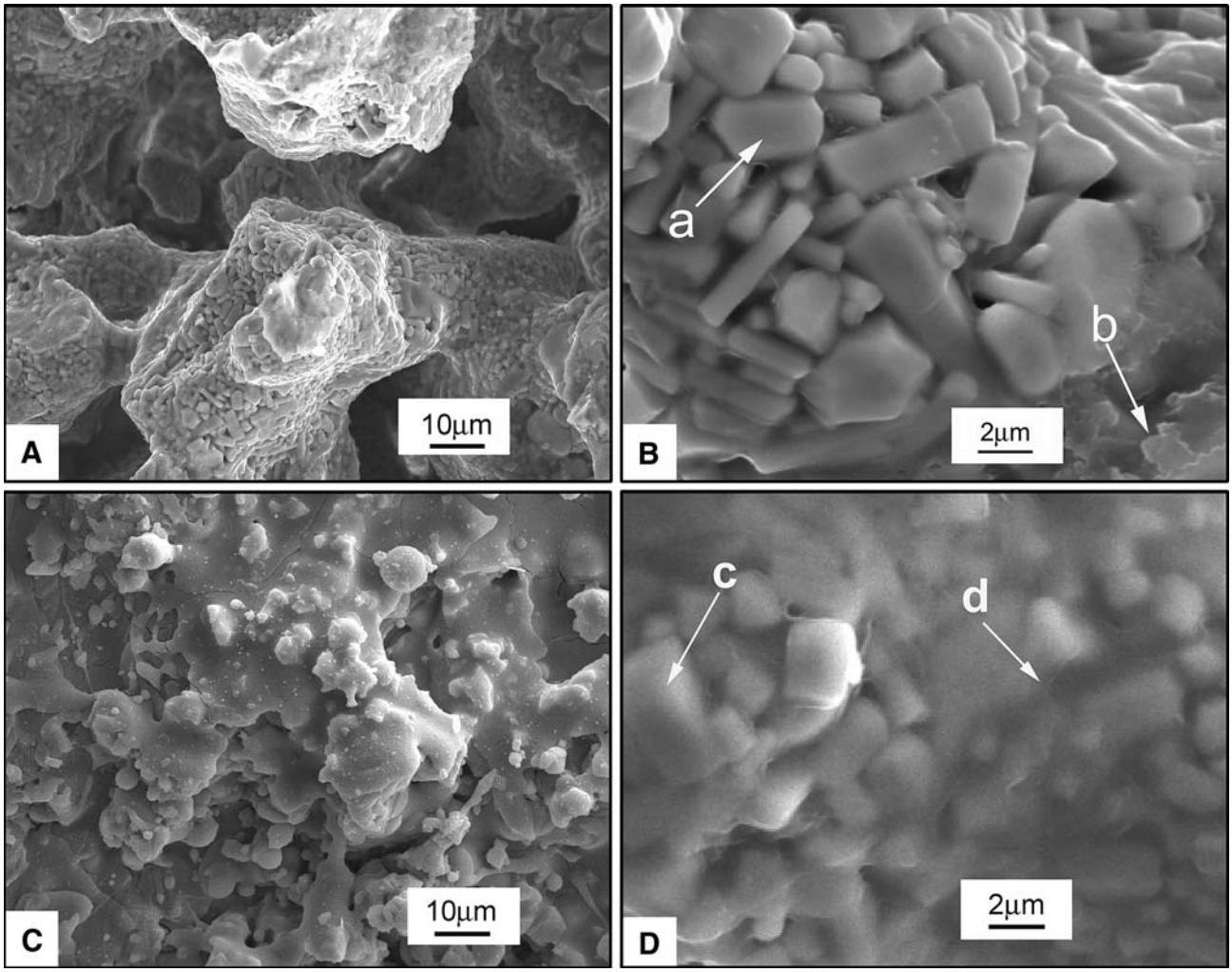

Fig. 2 SEM morphologies of (A) the sintered CZS powder and (B) higher magnification of (A), (C) as-sprayed CZS coating and (D) higher magnification of (C), (E) EDS of a, c points and (F) EDS of b, d points

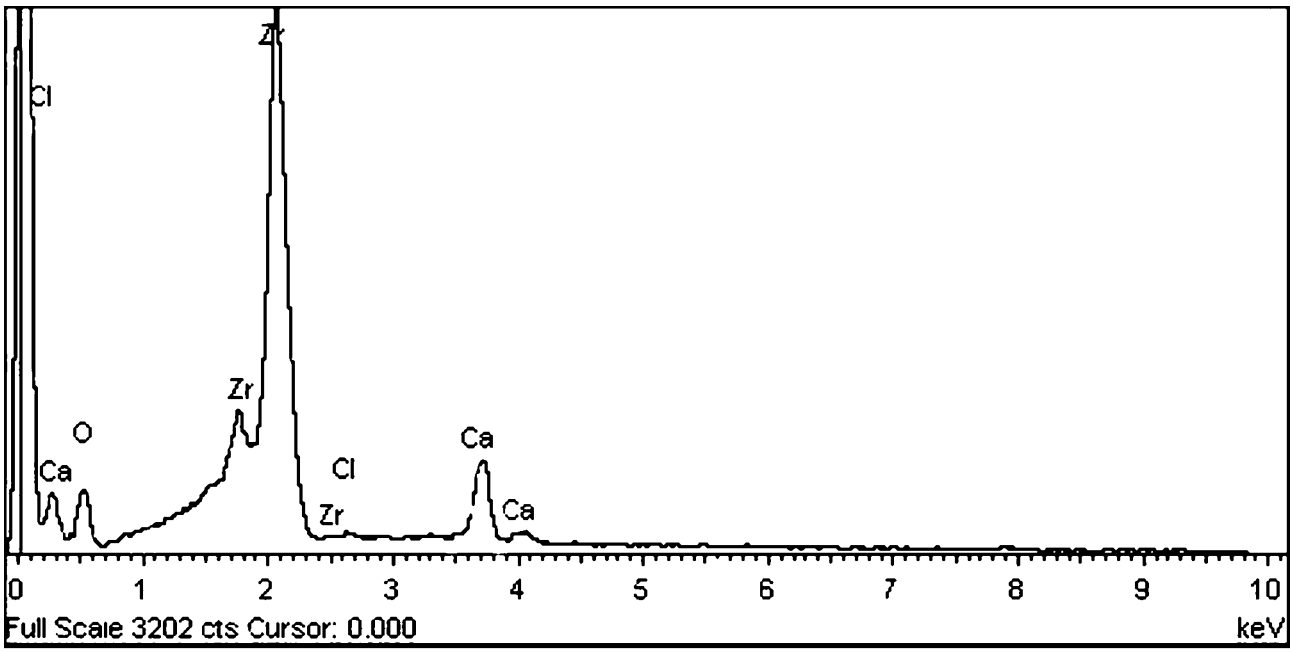

E

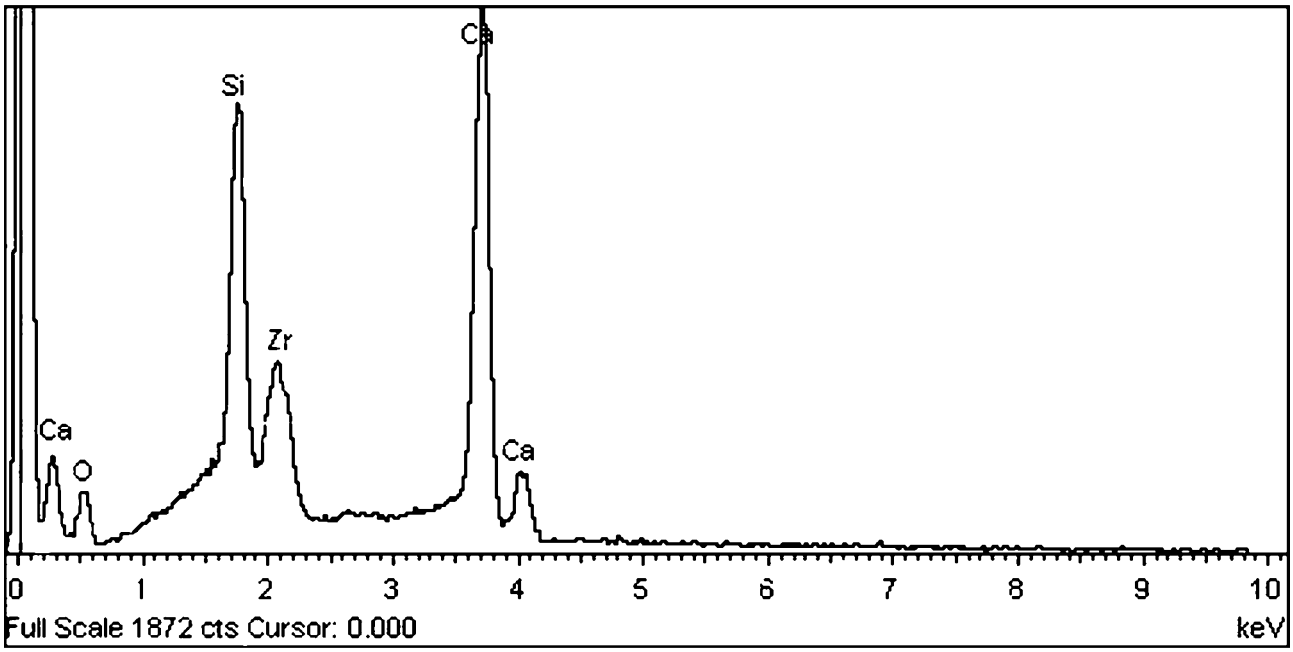

F

Fig. 2 continued

CZS coating was explained by the large content of zirconia in the CZS. Since the similar thermal expansion coefficient with titanium alloy substrate and high strength, good toughness (Ref 25), the bond strength of the plasma sprayed ZrO_2 coating is as high as 60.5 ± 2.6 MPa when the thickness of the coating is 200 μm (Ref 26).

It is known that bioactive materials bond to living bone via formation of a biologically active bone-like apatite layer (Ref 27) on their surfaces. The formation of apatite is an essential requirement to chemically bond to bone to some extent (Ref 28-30). For CZS coating, because of the existence of silicate salts and gradual release of calcium ions, apatite was formed on the surface after immersion in SBF. It implies that the coating possesses the potential to chemically bond to bone tissue when it is implanted. The well adhesion and proliferation behavior of the canine MSCs cultured on the coating also demonstrated the good in vitro cytocompatibility of the CZS.

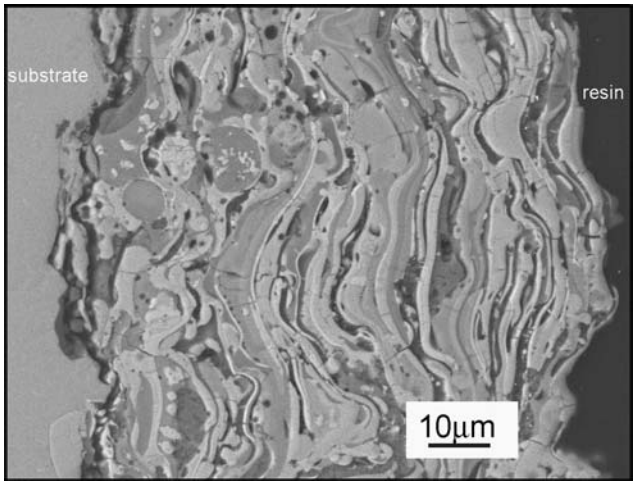

Fig. 3 Cross-sectional morphology of the as-sprayed CZS coating

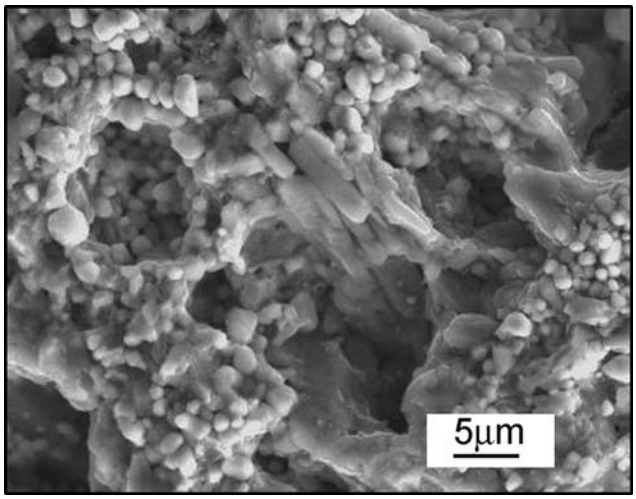

Fig. 4 Surface morphology of the CZS coating after immersion in Tris-HCl buffer for 30 days

5. Conclusions

CaO-ZrO_2-SiO_2 powder was chemically synthesized by employing the decalcification reaction between calcia partially stabilized zirconia and silica. The obtained powder was coated onto a Ti-6Al-4V substrate by air plasma spraying for potential application in biomedicine. The coating showed not only good bonding strength with titanium alloy substrate (31.8 ± 4.7 MPa) but also high stability in Tris-HCl buffer. In vitro bioactivity results showed that apatite was formed on the coating surface after 14 days immersion in SBF, implying that the coating possesses the potential to chemically bond to bone tissue. The canine marrow stem cells adhered, spread well on the coating surface and displayed very close proliferation behavior with those on HC. All these results suggest that the CZS coating possesses good cytocompatibility and potential application in biomedicine.

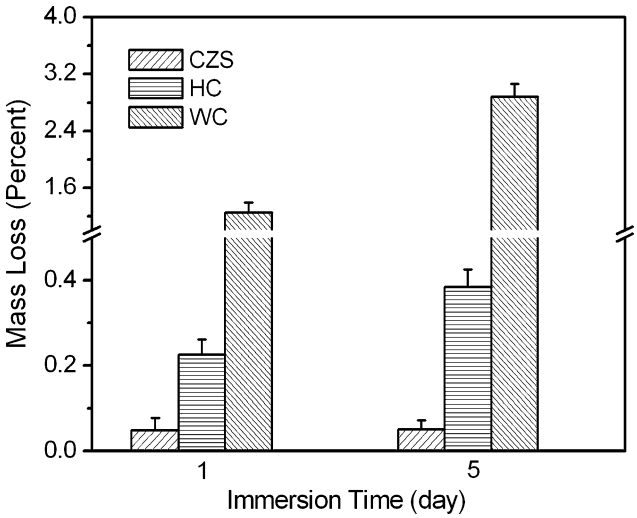

Fig. 5 Dissolution percent after immersion in Tris-HCl buffer for different immersion duration

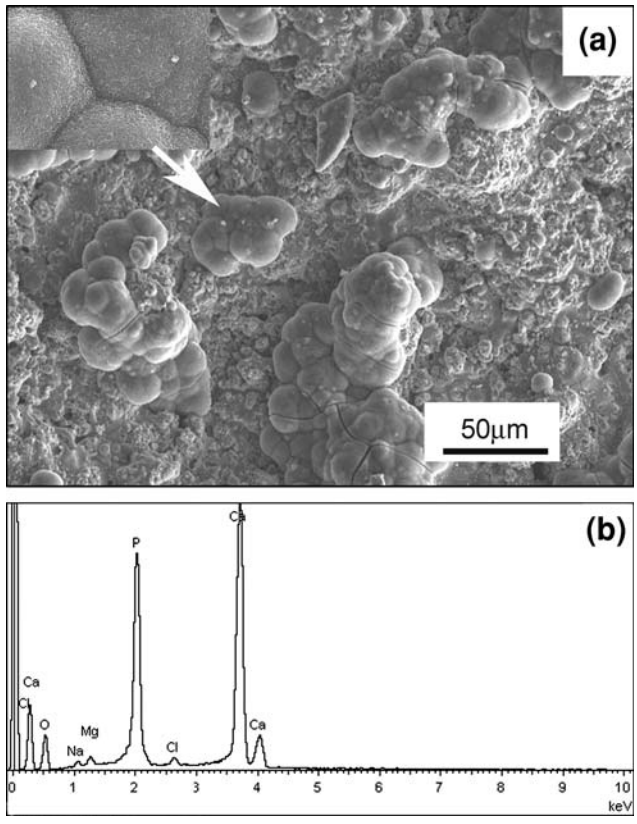

Fig. 6 Surface morphologies of (a) the CZS coating after immersion in SBF for 14 days and (b) EDS of the deposited layer

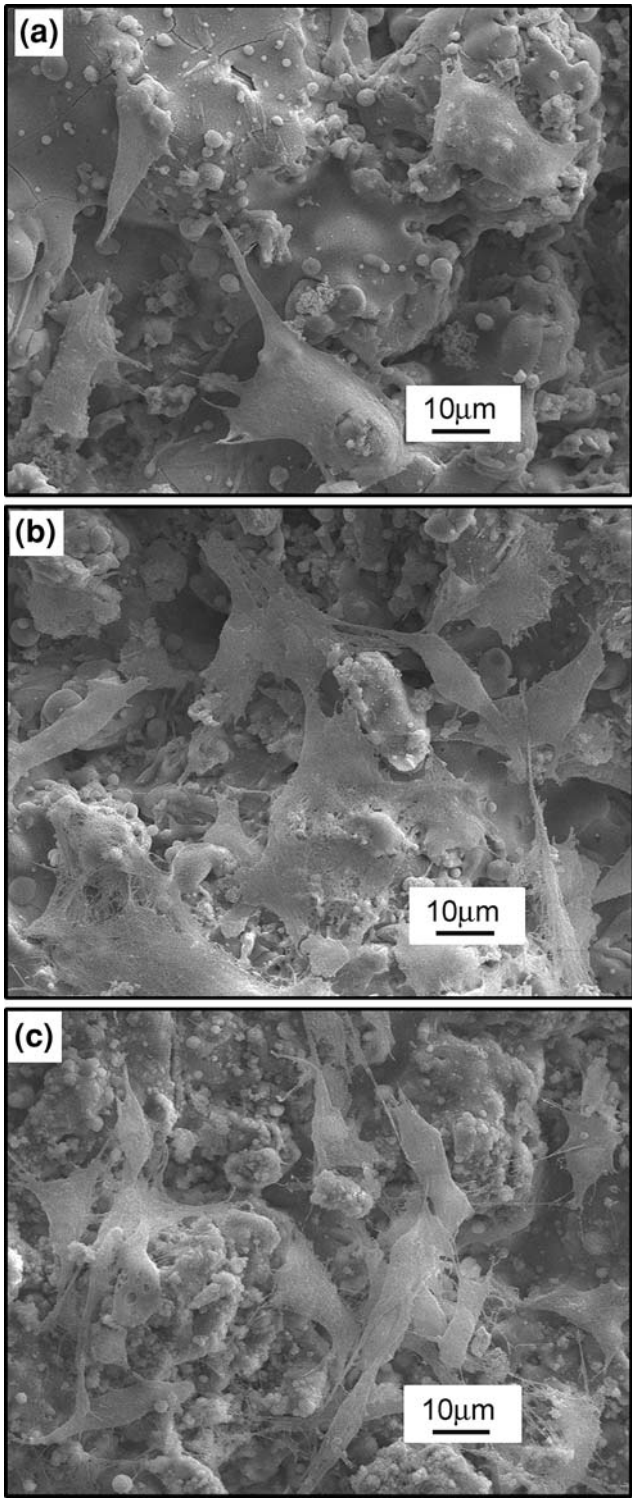

Fig. 7 SEM micrographs showing the morphologies of the seeded cells on the CZS coating surface: (a) after 2 days, (b) after 4 days and (c) after 6 days

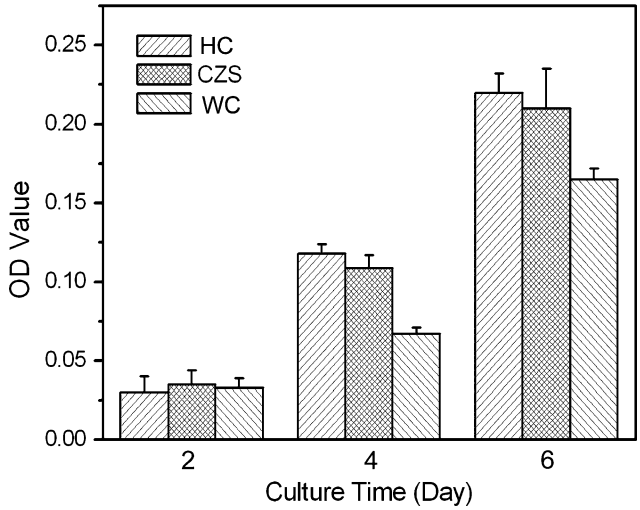

Fig. 8 Proliferation of MSCs (MTT assay) on the CZS coating surface (compared with those on the HC and WC surfaces)

References

1. L. Hench, Bioceramics, *J. Am. Ceram. Soc.*, 1998, **81**, p 1705-1728
2. Y. Tsui, C. Doyle, and T. Clyne, Plasma Sprayed Hydroxyapatite Coatings on Titanium Substrates Part 1: Mechanical Properties and Residual Stress Levels, *Biomaterials*, 1998, **19**, p 2015-2029
3. J. Breme, Y. Zhou, and L. Groh, Development of a Titanium Alloy Suitable for an Optimized Coating with Hydroxyapatite, *Biomaterials*, 1995, **16**, p 239-244
4. W. Xue, X. Liu, X. Zheng, and C. Ding, In Vivo Evaluation of Plasma-Sprayed Wollastonite Coating, *Biomaterials*, 2005, **26**, p 3455-3460
5. Y. Xie, X. Liu, C. Ding, and P. Chu, Bioconductivity and Mechanical Properties of Plasma-Sprayed Dicalcium Silicate/Zirconia Composite Coatings, *Mater. Sci. Eng. C*, 2005, **25**, p 509-515
6. P. De Aza, J. Fernández-Pradas, and P. Serra, In Vitro Bioactivity of Laser Ablation Pseudowollastonite Coating, *Biomaterials*, 2004, **25**, p 1983-1990
7. N. Claussen, Fracture Toughness of Al_2O_3 with an Unstabilized ZrO_2 Dispersed Phase, *J. Am. Ceram. Soc.*, 1976, **59**, p 49-51
8. D. Green, Critical Microstructures for Microcracking in Al_2O_3/ZrO_2 Composites, *J. Am. Ceram. Soc.*, 1982, **65**, p 610-614
9. M. Ruhle, A. Evans, R. Mcmeeking, and P. Charalambides, Microcrack Toughening in Alumina/Zirconia, *Acta Metall.*, 1987, **35**, p 2701-2710
10. B. Chou, E. Chang, S. Yao, and J. Chen, Phase Transformation During Plasma Spraying of Hydroxyapatite–10 wt%-Zirconia Composite Coating, *J. Am. Ceram. Soc.*, 2002, **85**, p 661-669
11. J. Wu and T. Yeh, Sintering of Hydroxyapatite/Zirconia Composite Materials, *J. Mater. Sci.*, 1988, **23**, p 3771-3777
12. K. Ioku, S. Somiya, and M. Yoshimura, Hydroxyapatite Ceramics with Tetragonal Zirconia Particles Dispersion Prepared by HIP Postsintering, *J. Jpn. Ceram. Soc.*, 1991, **99**, p 196-203
13. T. Kasuga, K. Nakajima, T. Uno, and M. Yoshida, Preparation of Zirconia Toughened Bioactive Glass/Ceramic Composite by Sinterhot Isostatic Pressing, *J. Am. Ceram. Soc.*, 1992, **75**, p 113-117
14. T. Kasuga, M. Yoshda, A. Ikushima, M. Tuchiya, and H. Kusakari, Stability of Zirconia-Toughened Bioactive Glass/Ceramics: In Vivo Study Using Dogs, *J. Mater. Sci.*, 1993, **4**, p 36-39

15. S. Hulbert, *The Use of Alumina and Zirconia in Surgical Implants: An introduction to Bioceramics*, L. Hench and J. Wilson, Ed., Word Scientific Publishing Co, Singapore, 1993, p 25-40
16. H. Lang and T. Mertens, The Use of Human Osteoblast Like Cells as an *In Vitro* Test System for Dental Materials, *J. Oral Maxillofac. Surg.*, 1990, **48**, p 606-611
17. I. Dion, L. Bordenave, F. Lefebvre, R. Bareille, C. Baquey, J. Monties, and P. Havlik, Physico-Chemistry and Cytotoxicity of Ceramics, *J. Mater. Sci.*, 1994, **5**, p 18-24
18. T. Tateishi, K. Hyodo, K. Kondo, and K. Miura, Simulator Test of Artificial Joints, *Mater. Sci. Eng. C*, 1994, **1**, p 121-125
19. S. Colin, B. Dupre, and C. Gleitzer, Decalcification of Stabilized Zirconia by Silica and Some Other Oxides, *J. Eur. Ceram. Soc.*, 1992, **9**, p 389-395
20. C. Ohtsuki, T. Kokubo, and T. Yamamuro, Mechanism of Apatite Formation on $CaO–SiO_2–P_2O_5$ Glasses in a Simulated Body Fluid, *J. Non-Cryst. Solids*, 1992, **143**, p 84-92
21. ASTM C633, Standard Method of Test for Adhesive or Cohesive Strength of Flame-Sprayed Coatings, *19th Annual Book of ASTM Standards*, Part 17, ASTM, Philadelphia, PA, 1969, p 636-642
22. X. Zheng, M. Huang, and C. Ding, Bond Strength of Plasma-Sprayed Hydroxyapatite/Ti Composite Coatings, *Biomaterials*, 2000, **21**, p 841-849
23. Y. Yang and E. Chang, Influence of Residual Stress on Bonding Strength and Fracture of Plasma-Sprayed Hydroxyapatite Coatings on Ti–6Al–4V Substrate, *Biomaterials*, 2001, **22**, p 1827-1836
24. J. Yeo, S. Choi, J. Kim, J. Lee, and Y. Jung, Thermal Reaction Behavior of $ZrSiO_4$ and $CaCO_3$ Mixtures for High-Temperature Refractory Applications, *Mater. Sci. Eng. A*, 2004, **368**, p 94-102
25. H. Hayashi, T. Saitou, N. Maruyama, H. Indba, K. Kawamura, and M. Mori, Thermal Expansion Coefficient of Yttria Stabilized Zirconia for Various Yttria Contents, *Solid State Ionics*, 2005, **176**, p 613-619
26. H. Zhou, F. Li, B. He, J. Wang, and B. Sun, Air Plasma Sprayed Thermal Barrier Coatings on Titanium Alloy Substrates, *Surf. Coat. Technol.*, 2007, **201**, p 7360-7367
27. L. Hench and A. Clark, Adhesion to Bone, *Biocompatibility of Orthopedic Implants*, Vol 2, D. Williams, Ed., CRC Press, Boca Raton, FL, 1982, p 129-170
28. T. Kokubo, Recent Progress in Glass-Based Materials for Biomedical Applications, *J. Ceram. Soc. Jpn.*, 1991, **99**, p 965-973
29. L. Hench, Bioceramics: From Concept to Clinic, *J. Am. Ceram. Soc.*, 1991, **74**, p 1487-1510
30. T. Kokubo, Bioactive Glass–Ceramics: Properties and Applications, *Boimaterials*, 1991, **12**, p 155-163